SAGE CALCULATIONS OF THE TSUNAMI THREAT FROM LA PALMA

Galen Gisler
Los Alamos National Laboratory and University of Oslo
Robert Weaver
Los Alamos National Laboratory,
Michael L. Gittings
Science Applications International
Los Alamos, NM, USA

ABSTRACT

With the LANL multiphysics hydrocode SAGE, we have performed several two-dimensional calculations and one three-dimensional calculation using the full Navier-Stokes equations, of a hypothetical landslide resembling the event posited by Ward and Day (2001), a lateral flank collapse of the Cumbre Vieja Volcano on La Palma that would produce a tsunami. The SAGE code has previously been used to model the Lituya Bay landslide-generated tsunami (Mader & Gittings, 2002), and has also been used to examine tsunami generation by asteroid impacts (Gisler, Weaver, Mader, & Gittings, 2003). This code uses continuous adaptive mesh refinement to focus computing resources where they are needed most, and accurate equations of state for water, air, and rock. We find that while high-amplitude waves are produced that would be highly dangerous to nearby communities (in the Canary Islands, and the shores of Morocco, Spain, and Portugal), the wavelengths and periods of these waves are relatively short, and they will not propagate efficiently over long distances.

1. INTRODUCTION

Tsunami that affect the Atlantic Ocean are much less frequent than those that affect the Pacific and Indian Oceans, nevertheless they do occur. The 1 November 1755 Lisbon earthquake (*e.g.* Chester 2001, Mader 2001) is an example of an event that produced an ocean-wide tsunami. There are other potential tsunamigenic hazards in the Atlantic, including submarine volcanoes (*e.g.* Kick-em Jenny in the Eastern Caribbean, Smith & Shepherd, 1993, 1995), submarine landslides associated with deep ocean trenches and continental slopes, and subaerial landslides, particularly from any of the steep-sided volcanic islands in the Atlantic. Though the frequency of such events is low, the establishment of an Atlantic Tsunami Warning System would be justified for the protection of the millions of people populating Atlantic shores.

This report summarizes the findings of our two-dimensional and three-dimensional simulations of a hypothetical tsunami resulting from the lateral flank collapse of the Cumbre Vieja volcano on the island of La Palma in the Canary Islands. Such a collapse, similar to the Mt St Helens collapse in May 1980, could send as much as 500 cubic kilometers of rock in the form of a debris avalanche into the Atlantic Ocean, triggering a tsunami (Ward and Day 2001). We do not here address the likelihood of such a flank collapse or its eventual magnitude, other than to bracket the magnitude as part of a parameter study we have undertaken. We do note, however, that the Ward and Day work has been met with considerable skepticism in the scientific community. Mader (2001), Pararas-Carayannis (2002), and Wynn and Masson (2003) argue against this, respectively, because a long-period wave is unlikely to result even from a total collapse, because such a total collapse is held to be unlikely, and because the record of turbidite deposits in the vicinity of the Canary Islands does not support such catastrophic events in the past.

Bathymetry of the region around the Canary Islands is essential for the accuracy of this project, and we have requested from the Spanish Government multi-beam bathymetry data that will help resolve the nature and magnitude of the long-range danger from an event of this type. The report presented here is based on the much poorer data available in the public domain. The limited resolution of these data is an important limitation on the quality of the three-dimensional tsunami simulations, and we hope to repeat these calculations when better data become available.

Three-dimensional Navier-Stokes simulations are needed in order to predict the wave radiation pattern that results from a tsunamigenic event. Shallow-water wave theory and other approximations do reasonably well at long-distance propagation given an accurate description of the wave form that results from from an event, but the production of the wave form itself requires accurate calculation of the complex interaction between the water and the perturbing medium. Entrainment, turbulence, and turbidity currents are all important.

While three-dimensions and good bathymetry are needed for calculating the radiation pattern, two-dimensional calculations (depth and longitudinal distance) can predict the wavelengths and periods of the wave trains that are produced from the triggering event, while greatly overestimating amplitudes. Since two-dimensional calculations are relatively inexpensive and can be done at high resolution, parameter studies work well to determine how the observed characteristics of the wave depend on the physical inputs of the event.

2. THE SAGE HYDROCODE

The SAGE hydrocode is a multi-material adaptive-grid Eulerian code with a high-resolution Godunov scheme originally developed by Michael Gittings for Science Applications International (SAIC) and Los Alamos National Laboratory (LANL) under the Department of Energy's program in Advanced Simulation and Computing, or ASC. It solves the full set of compressible Navier-Stokes equations, and uses continuous adaptive mesh refinement (CAMR), by which we mean that the decision to refine the grid is made for each cell at every cycle throughout the problem run, depending on gradients in physical properties. With this technique, large computational volumes with substantial differences in scale can be simulated at low cost.

Each cell in the computational volume can contain all materials defined in the problem with different equations of state and rheology. We use the LANL SESAME tables of material properties for air and basalt, but for water we used a more sophisticated table that includes a good treatment of the vapor dome and phase transitions from SAIC. Detailed testing of the water equation of state shows excellent agreement with experimental results.

The boundary conditions we use in these tsunami calculations are designed to allow unhindered outflow of waves and material. This is accomplished by the use of “freeze regions” around the edges of the computational box, which are updated normally during the hydrodynamic step, then quietly restored to their initial values of pressure, density, internal energy, and material properties before the next step. This technique has proven to be extremely effective at minimizing the deleterious effects of artificial reflections.

3. TWO-DIMENSIONAL SIMULATIONS OF CHARACTERISTIC SUBAERIAL LANDSLIDES

A simple schematic slide geometry was suggested to us by Simon Day (private communication) as a two-dimensional representation of likely slides at Cumbre Vieja. The slide region is wedge shaped, deepest at the top, tapering to a point or toe at the bottom, and having an offset towards the back (east) side of the peak (see Figure 1). Below this, to the bottom of the computational grid, is a rigid reflecting boundary representing the unchanging basement rock of La Palma. The motion is initiated solely by the gravitational acceleration of the fluidized rock (with the density of basalt) in the slide region. The two-dimensional calculations are done in Cartesian coordinates, thus effectively assuming infinite extent in the direction perpendicular to the simulation plane.

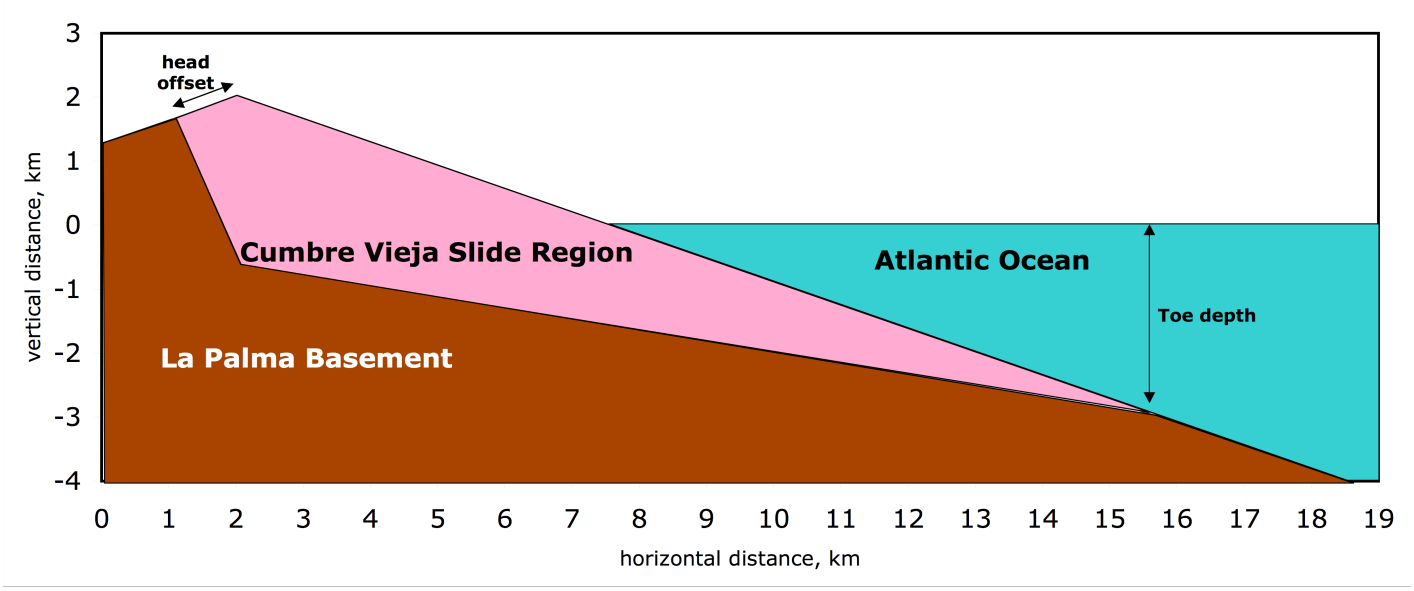

Figure 1. Schematic setup for our two-dimensional runs. The pink material labeled "Cumbre Vieja Slide Region" is the fluidized rock that accelerates under gravity and slides down into the ocean (blue). The brown region labeled "La Palma Basement" is an internal reflective boundary. The setup shown here is for run Dth31, with toe depth 3 km and head offset 1 km. Varying these two numbers constituted our parameter study.

We ran four variants of this geometry, with the toe at depths of 2 and 3 kilometers, and the head offset at 1 and 2 kilometers. These runs are named so as to indicate the toe depth and head offset; thus Dth21 has toe depth 2 km and head offset 1 km, and Dth32 has toe depth 3 km and head offset 2 km. The total volumes, assuming a 25 kilometer perpendicular extent are: run Dth21, 308 km^3; run Dth22, 332 km^3; run Dth31, 473 km^3; and run Dth32, 503 km^3. These are all run with a finest resolution of 15 meters, certainly adequate to resolve the (hundreds of meters) initial wave heights expected. This resolution also enables the tracking of turbidity currents as the fluidized basalt slide material mixes with the water, and can help diagnose the energy trades that occur between the slide material and the water, and between the water and the atmosphere. These runs have on the order of 300,000 cells, and ran for a few hundred hours on 10–20 processors of a Linux Opteron cluster at Los Alamos.

An impression of the character of the wave is obtained from a graphic rendering of density at a time early in the calculation (Fig. 2). This figure shows a small portion of the computational domain; the box extends to the right out to a distance of 120 km from the island. The fluidized rock has accelerated into the water, initially producing a crater, then a substantial wave. The slide speed in this inviscid calculation reaches as high as 190 m/s before decelerating as the slide gives up energy to the water. The peak slide speed almost matches the shallow-water wave speed ($\sqrt{gd}$ ~ 198 m/s) so the bullnose of the slide material falls behind the water wave only gradually, and continues to pump energy into the water wave. A single broad wave is thus produced, with trailing higher-frequency components that are excited by the eddy currents in the turbulent mixing and entrainment of slide material and water. As the slide material decelerates, the water wave detaches and outruns

it, but no further low-frequency modes are produced.

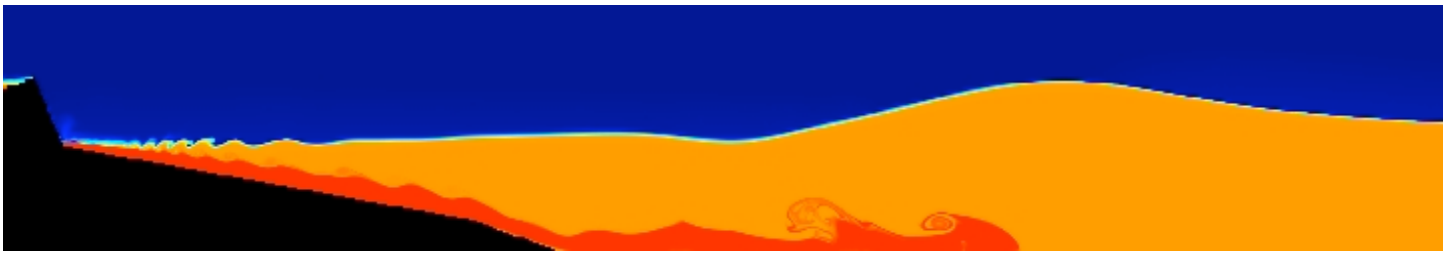

Figure 2. Density raster plot in our 2d run Dth32 at a time of 180 seconds after the start of the slide. The reflective region representing the unchanging basement of La Palma is at left in black, the basalt fluid slide material is red, water is orange, and air is blue. Intermediate shades represent the mixing of fluids, in particular the turbidity currents mixing water and basalt are readily apparent. The water wave leads the bullnose of the slide material by a small amount; the forward-rushing slide material (with a velocity of 190 meters/second almost matching the wave velocity) continues to pump energy into the wave. The wave height at this time is 1500 meters, and the wavelength is roughly 60 km. This figure has a width of 50 km, representing less than half of the computational domain, which extends 120 km to the right.

We measured maximum wave heights, wavelengths, periods, and wave speeds for these four runs, and summarize them in Table I. These quantities were obtained by inspecting the trajectories of massless Lagrangian racer particles initially placed along the surface of the water. Graphs of vertical (y) and horizontal (x) position as functions of time for the tracers in run Dth32 are presented in Figure 3.

Table I. Important characteristics of the two-dimensional runs

run	slide volume (km^3)	max wave height (m)	wavelength (km)	period (s)	wave speed (m/s)
Dth21	308	1303	48	252	192
Dth22	332	1327	48	250	192
Dth31	473	1474	53	262	202
Dth32	503	1508	61	291	209

The wave period and wavelength depend only weakly on the slide volume (roughly as the 1/3 and 1/2 power, respectively), but both the period and wavelength of these waves are short compared to those of teletsunamis commonly observed in the Pacific or Indian Ocean. The long-distance propagation of these waves will not be as effective as classical long-wavelength tsunamis. We do not see low-frequency components arising in the water wave, though a cascade to higher frequency is apparent in the tracer plots of Figure 3. Concerned that our 120 km box length prevented the development of lower frequency waves, we repeated the Dth31 calculation with a box length of 240 km, producing results that were identical in all respects.

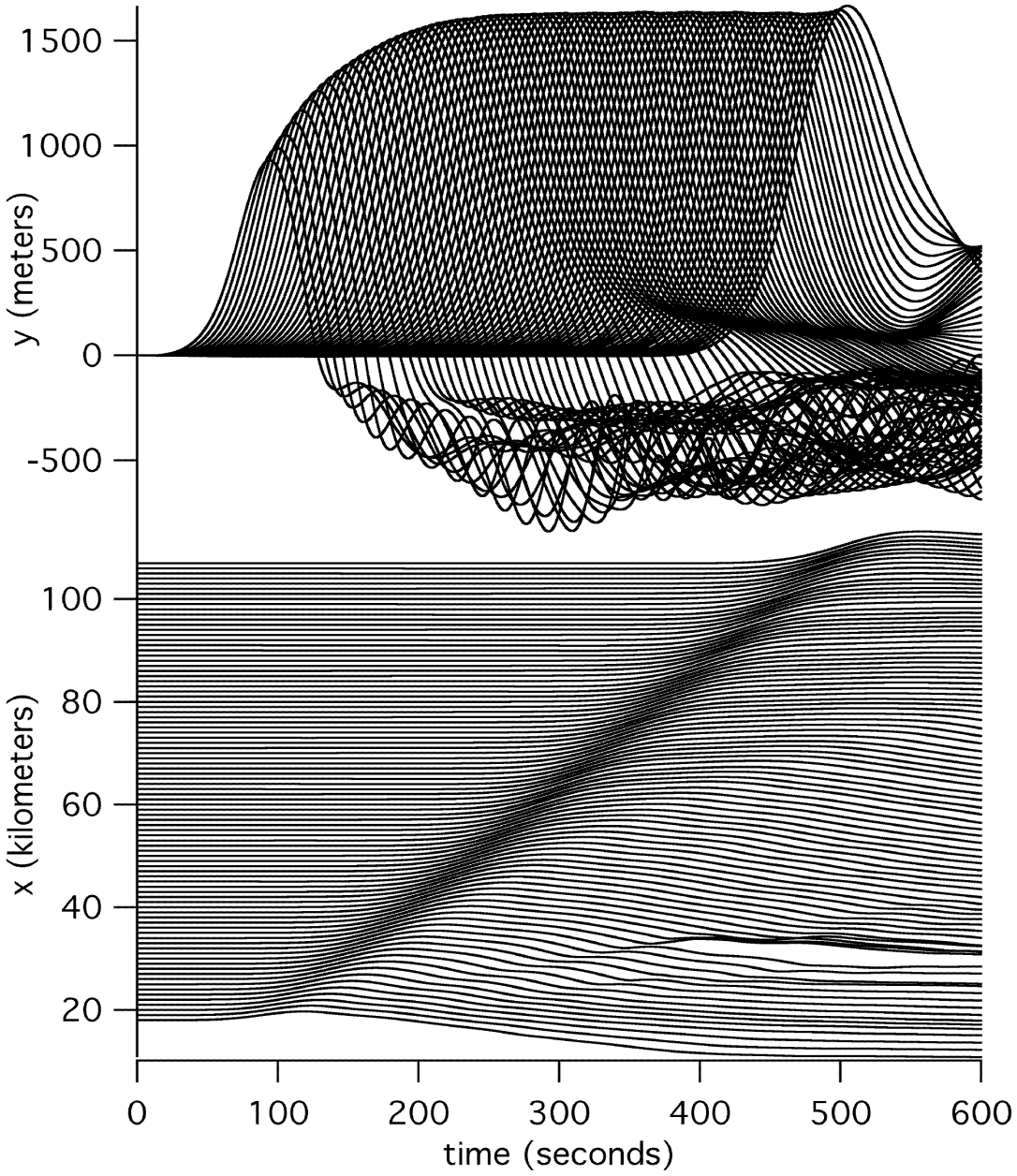

Figure 3. Tracer positions as a function of time in run Dth32. Top is vertical position, bottom is horizontal position. The wave velocity is measured directly from the bottom plot, and amplitude and period are estimated from the upper plot. Although the massless Lagrangian tracers are placed initially on the water surface, they do not remain on the surface but follow the fluid in the computational cell in which they happen to reside at any given time. Therefore they tend to random-walk away from the surface into the body of the water. This accounts for the late-time under-surface tangle in the top plot towards late time.

It is very important to note that although these waves probably do not pose a significant danger to the western shores of the Atlantic Ocean, these large-amplitude waves will be very dangerous locally, *i.e.* to the

shores of other islands in the Canaries Archipelago and to mainland Africa and Europe.

For validation of the periods and wavelengths determined by SAGE, we turn to the example of the Ritter Island tsunami in Papua New Guinea in 1888, which was triggered by a debris avalanche following the eruption of the Ritter Island volcano (Ward and Day 2003). The geometry and mechanism are similar to those of the hypothetical La Palma event, but the slide cross-section is considerably smaller. We ran a calculation of Ritter Island with SAGE, and found a wave period of 180s, in agreement with the observations made at the time, see Figure 4 for the tracer plots. This period also accords with the 1/3-power volume scaling from the La Palma parameter study as mentioned above.

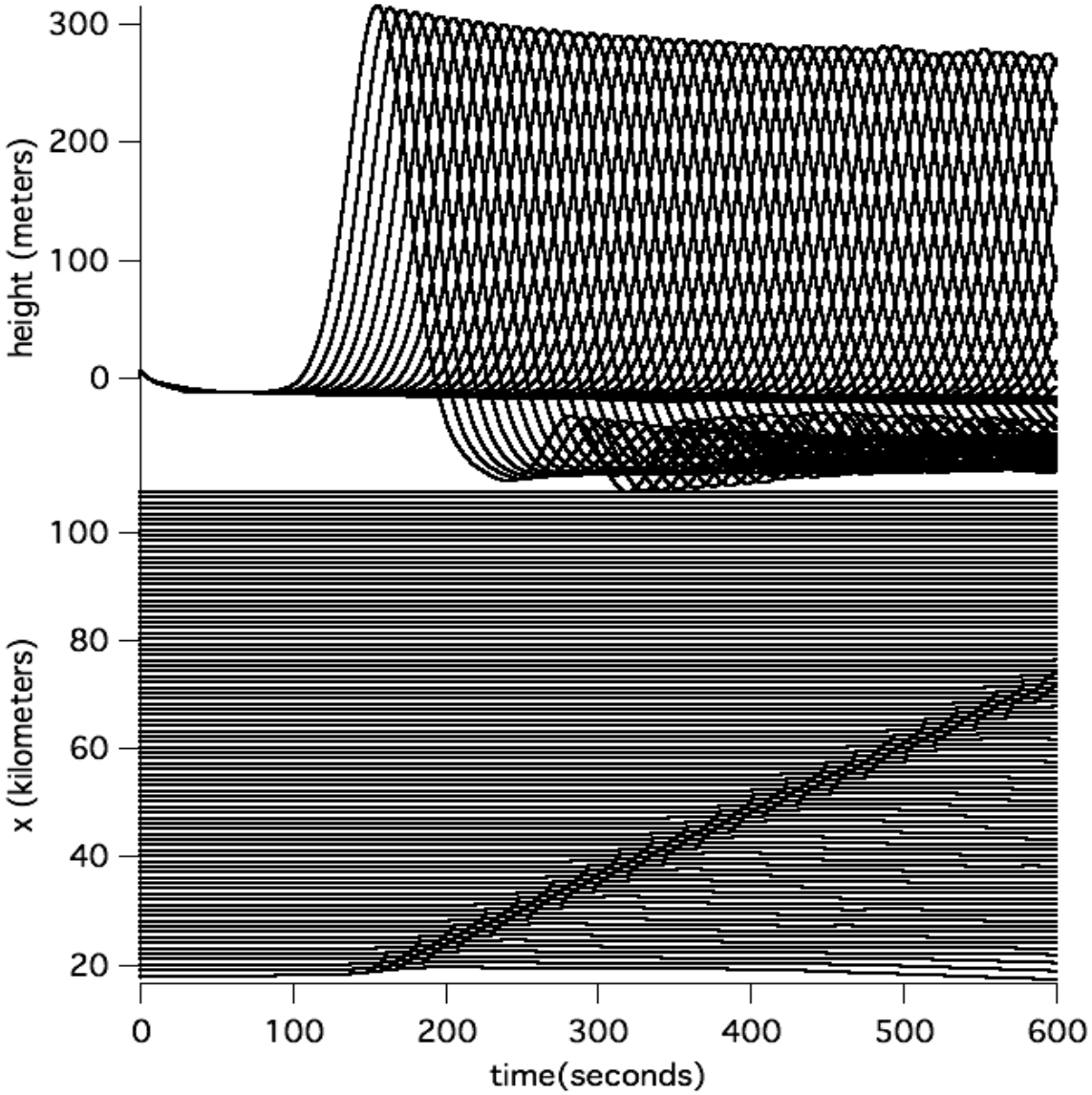

Figure 4. Tracer positions as a function of time in our Ritter Island simulation run. As in Figure 3, top is vertical position, bottom is horizontal position. The wave velocity is measured directly from the bottom plot, and amplitude and period are estimated from the upper plot.

Because the basalt slide is treated as an inviscid fluid in the calculations reported above, the speed and eventual reach of the slide material may be overestimated. To judge this, we preformed an additional set of calculations treating the rock slide as a plastic flow, with a shear modulus of 1 kBar and nominal yield stress, so that flow begins immediately. In Figure 5 we show comparisons of our Dth31 run with the plastic flow run Gth31, which is otherwise identical. We find that the slide is considerably slower in the plastic flow case. At 270 seconds, the time of the figure, the Dth31 slide has a horizontal velocity of 148 m/s, while the Gth31 slide has 131 m/s. Since these speeds are still possibly higher than expected, it may be that the plastic flow model would require a greater shear modulus to be realistic.

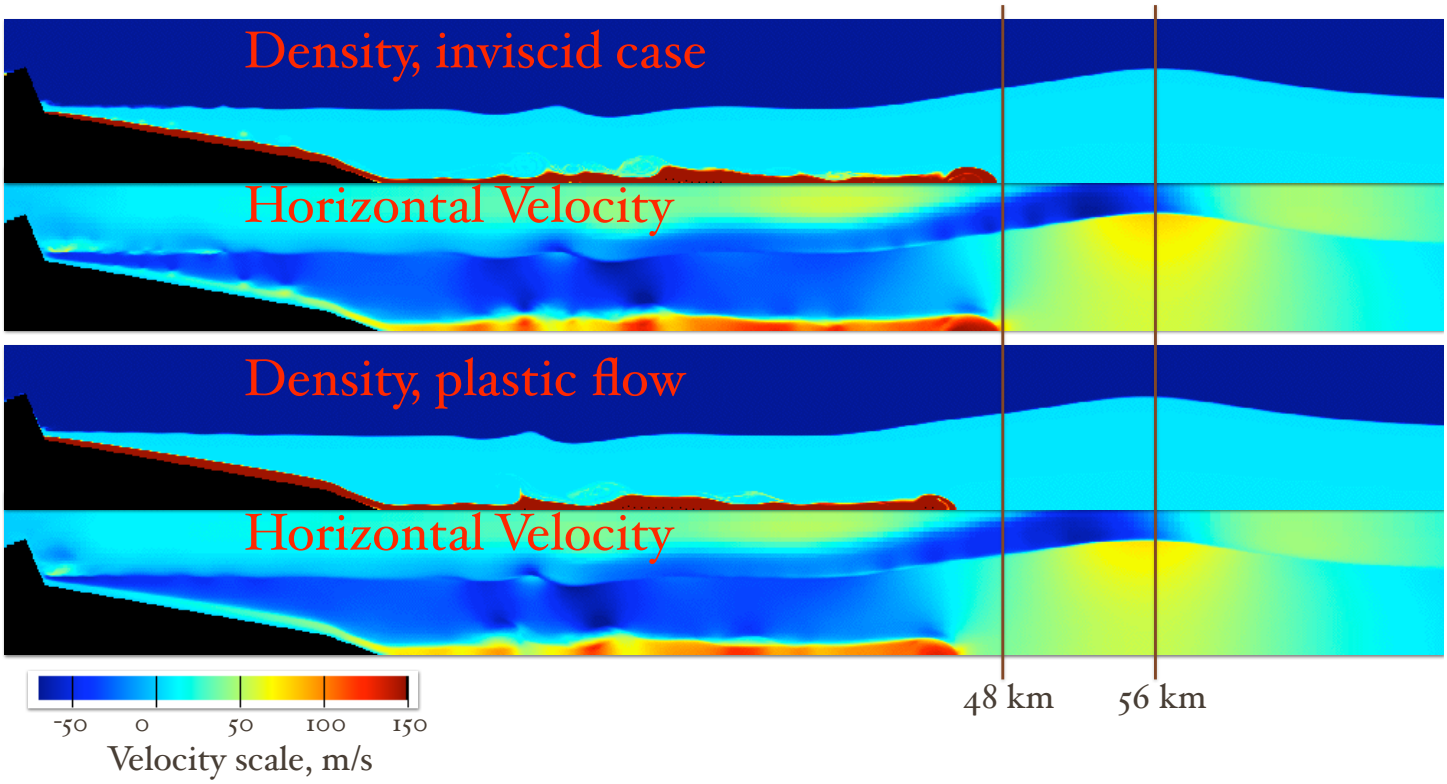

Figure 5. Comparison of the inviscid-slide calculation Dth31 with the plastic-flow slide calculation Gth31 at 270 seconds after the start of the calculation. The slide in Gth31 is significantly retarded in velocity and position with respect to the inviscid case, and the ripples in the basalt slide (which would represent turbidite layerings) are further apart and suppressed in amplitude. The maximum horizontal velocity of the slide material is 150 m/s in the inviscid case, 130 m/s in the plastic-flow case. The position and velocity of the water wave are unaffected. Note the strong velocity gradient across the water-air interface at and behind the wave crest in both cases. The Kelvin-Helmholtz instability will very likely cause the wave to degenerate further into high-frequency components. The amplitude of the wave in Gth31 is also very slightly less than in Dth31.

However, some landslides are well known to be quite runny, and may be lubricated by fragmentation and melt in the lower layers, or by acoustic fluidization as in sturzstroms (Collins and Melosh, 2003). Studies are underway to establish a good validation point. More relevant to observations of past landslides is the fact that

the plastic flow case produces larger eddies, and hence larger intervals between turbidite layers in the same landslide. Studies of turbidite layers in Hawaiian and Canary Island landslides (Wynn and Masson 2003) as well as for truly massive events such as Storegga, may prove useful for helping to untangle underwater slide dynamics. The position and speed of the water wave are the same in both calculations, but the amplitude is slightly less in the case with the debris avalanche treated as a plastic flow (1462 meters as compared with 1532 meters).

4. THREE-DIMENSIONAL SIMULATIONS OF A LA PALMA/CUMBRE VIEJA LANDSLIDE

The very high amplitudes found in our two-dimensional calculations are in the first place suspect because the Cartesian calculation geometry does not allow for dispersion in the transverse direction. A simple and inexpensive way to estimate the effect of transverse dispersion is by running a similar calculation in cylindrical coordinates, then this can further be checked by running a full three-dimensional calculation.

By way of illustration, then, we present in Figure 6 tracer particle plots for the two-dimensional Cartesian D31 and a two-dimensional cylindrical run with similar parameters. The maximum wave height is down by a factor 3, and the amplitude declines with distance from the source roughly as r^{-1} as expected.

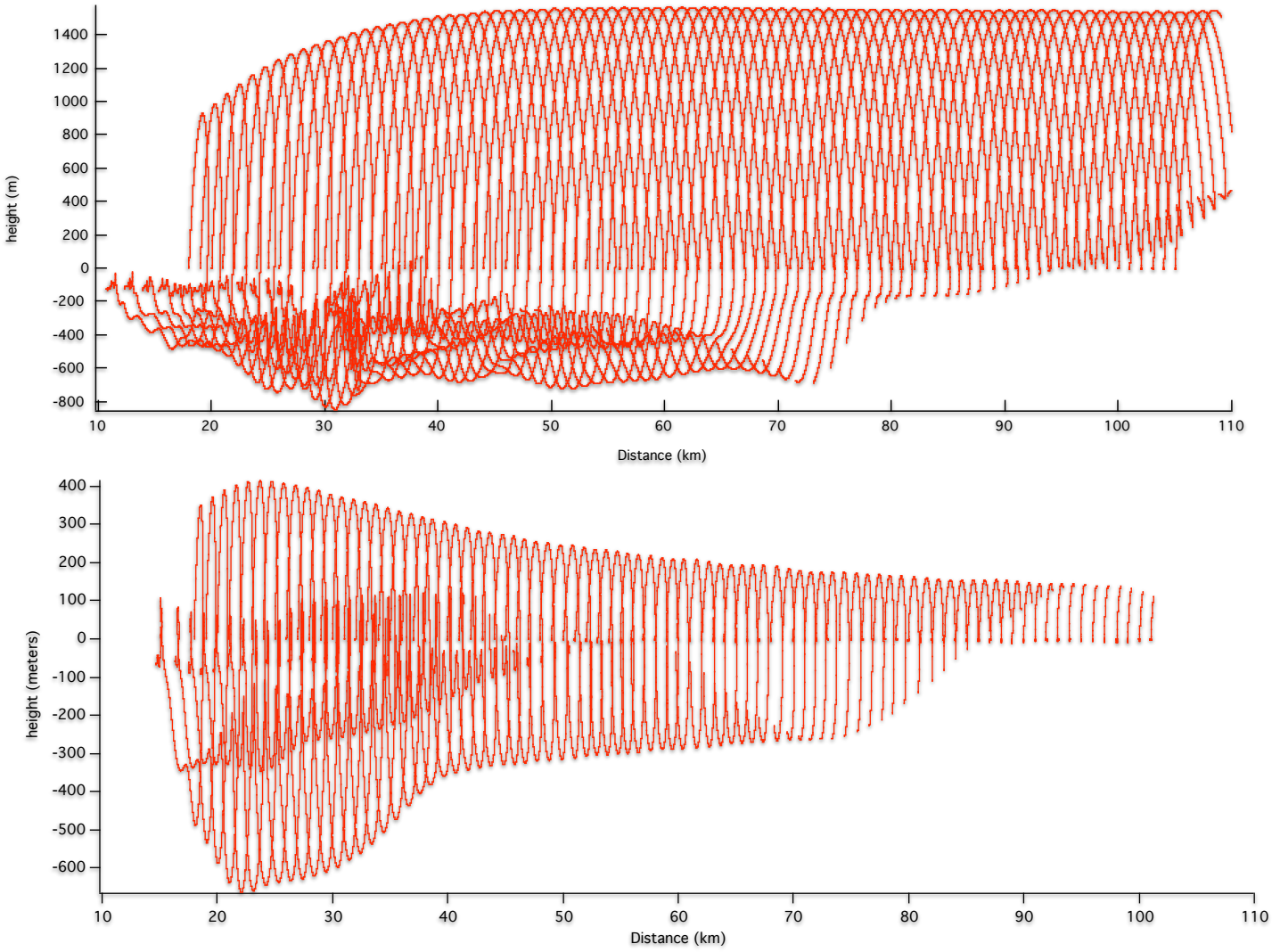

Figure 6. Comparison of tracer particle trajectories in the vertical plane for the Cartesian-geometry calculation Dth31 and the cylindrical-geometry-calculation Cth31. The maximum amplitude is less by a factor 3 in the latter case, and the expected r^{-1} decline with distance away from the source is observed.

Our single three-dimensional run of the hypothetical La Palma landslide uses publicly available bathymetry and topography from the web site of the USGS. Because the resolution of these data is so coarse (2 minutes, or roughly 4 kilometers), we've chosen much coarser resolution for this run, namely 125 meters. The slide region for this run was made by performing rather simple geometrical cuts on the crude topography to yield a volume in the range considered by Ward and Day, with no reference to actual geological features of the Cumbre Vieja volcano. Our slide has a volume of 375 km^3. This run has on order 60,000,000 cells, and requires 500 processors of a Linux Xeon cluster at Los Alamos. Because of the coarse resolution, we have so far used this run only to make a first pass at the radiation pattern of the tsunami that would result from the proposed slide. This radiation pattern, at a time of 209 seconds after the start of the gravity-initiated slide, is shown in Figure 7.

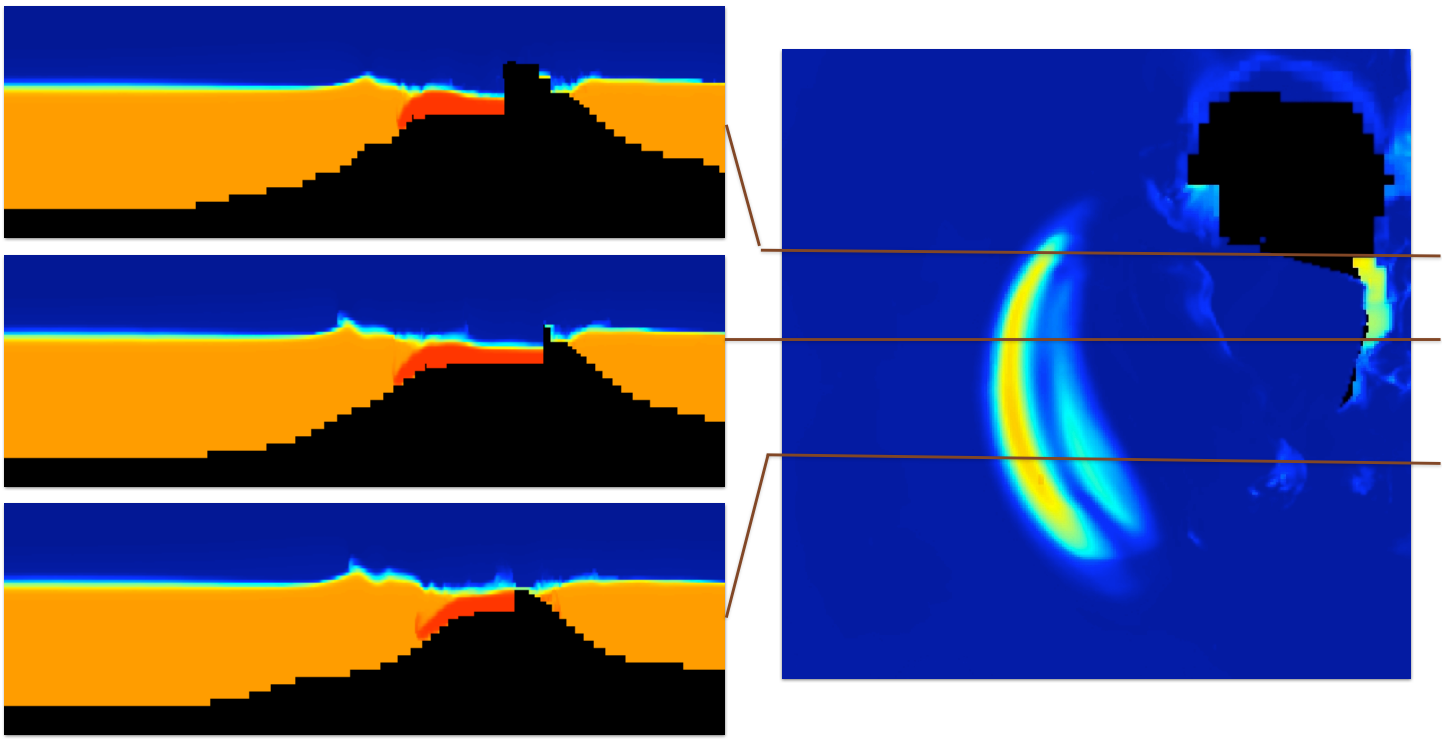

Figure 7. At right, a density raster plot in a horizontal slice through our 3d calculation at 500 meters altitude at a time of 209 seconds, and at left, three vertical slices through the same calculation at the positions indicated. The reflective region representing the island of La Palma is in black, and the original slide position has been vacated. Deep blue represents the density of air, orange the density of water, and shades in between indicate mixtures of air and water. The peak of the large-amplitude wave is directed towards the SSW, and a following crest is following in the same direction. A line extended through the peak strikes the northeast coast of South America. The vertical slices at left (exaggerated 5 times in the vertical direction) show that the highest wave is at the southern end of the slide. With more accurate bathymetry, we should be able to provide a fairly good prediction of the full radiation pattern. Note that there is considerable wave energy at this 500 meter level directed towards the other islands in the Canaries archipelago and toward the African and Spanish mainland, indicating the possibility of locally dangerous waves impinging on those shores.

In this three-dimensional run we find that the wave has even a shorter wavelength than we saw in the two-dimensional runs, but we await the high-quality bathymetry from the Spanish government before committing to this interpretation and evaluating quantitatively the threat to North America. It seems clear, nevertheless, that there is no significant wave energy directed towards the North Atlantic. If there is a long-distance threat from an event of this type, the regions most likely to be affected would be the Eastern Caribbean and the Northeastern Coast of South America. Considerable damage would be expected, however, in the Canaries, Morocco, Portugal and Spain if a large-scale collapse of Cumbre Vieja were to occur.

We make an attempt to estimate the distant effects by using the maximum height of the waves detected by our Lagrangian tracer particles as a function of distance from the source in our admittedly crude three-dimensional simulation. These simulation data are shown in Figure 8, which suggests a considerably stronger decline with distance than the r^{-1} decline seen in the cylindrically-symmetric run. The reasons for this difference may have to do with more degrees of freedom for the air/water and rock/water interaction instabilities, but the

coarseness of the resolution used in the three-dimensional calculation may also be a factor. In any case, we may use the r^{-1} decline seen in the cylindrical-geometry run and the $r^{-1.85}$ decline seen in the three-dimensional run to bracket extrapolations of the wave amplitudes expected in Surinam (towards which the strongest waves are evidently headed, from Figure 7) and Florida. For Surinam, at a distance of 4700 km from La Palma, the r^{-1} decline yields a wave height of about a meter, and the $r^{-1.85}$ decline yields a wave height of only about 2 cm. For Florida, at a distance of 6100 km, the r^{-1} decline yields a wave height of about 77 cm, and the $r^{-1.85}$ decline yields a wave height of only about 1.2 cm. Even the largest of these estimates is considerably smaller than the worrisome values given by Ward and Day (2001). Shoaling and distant focusing are of course omitted here, but are not expected to yield disastrous waves in any case.

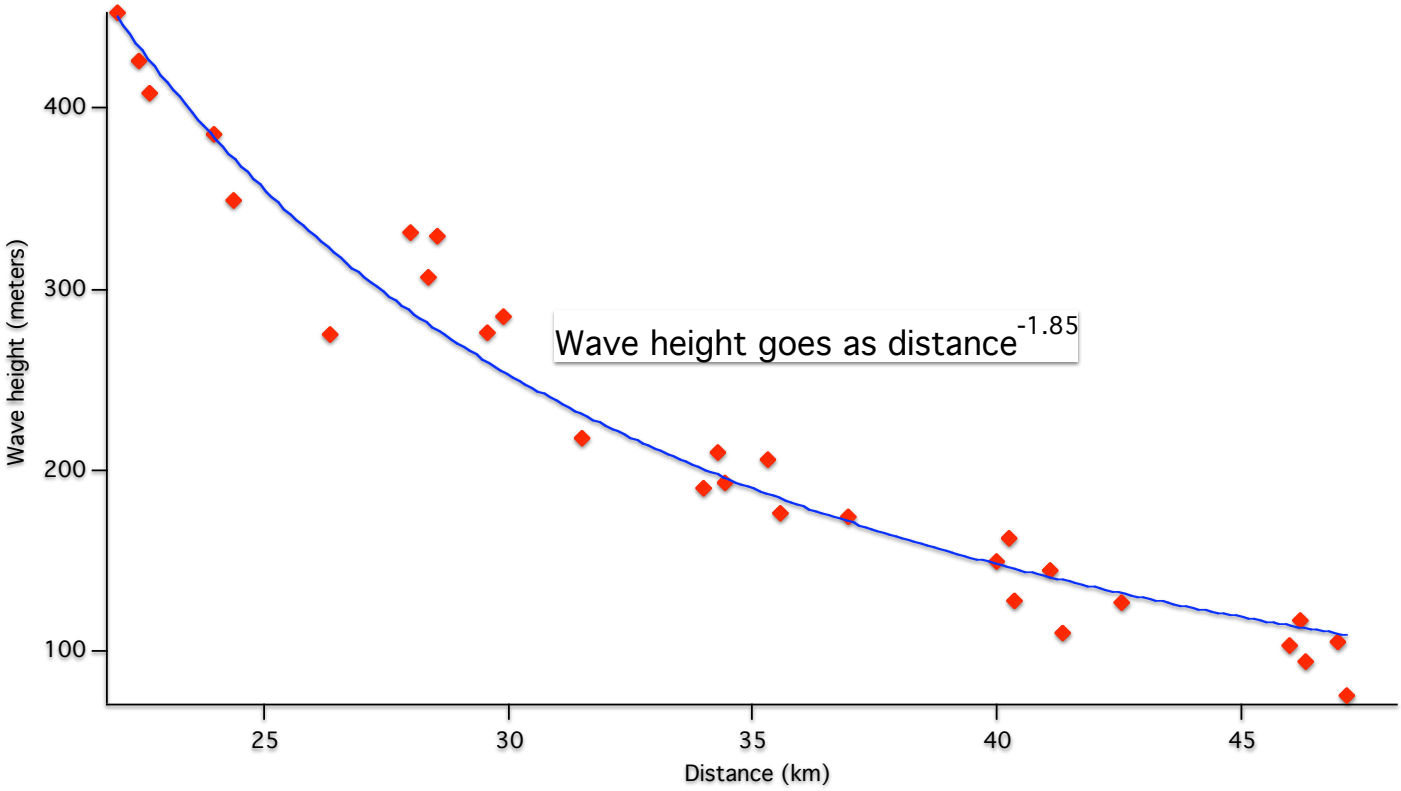

Figure 8. Maximum wave heights detected by our Lagrangian tracer particles as a function of distance away from the initial landslide peak, together with a best-fit power-law line giving a decline with distance as $r^{-1.85}$. If the long-distance wave propagation continues to decline in this way, the waves expected on the western shores of the Atlantic Ocean are unimportant.

5. FUTURE WORK

We intend to undertake new calculations in three dimensions of this scenario which will utilize the better bathymetric data of the Canary Islands furnished by the Spanish government. We have also enlisted the assistance of a group at Stanford University who have an incompressible flow solver together with a granular flow treatment for physics of the landslide itself. Granular flow and landslides are also a subject of intense

interest at the Centre for the Physics of Geological Processes at the University of Oslo, where one of us (Gisler) has recently moved, and are done there with finite-element and special-purpose methods focusing on fragmentation and lubrication effects. These calculations will complement the pure fluid, fully compressible solver in SAGE. Compressible-flow effects are indeed highly relevant in the very early stages of tsunami generation; but runs to longer physical times are more easily done with an incompressible solver, giving smooth transitions to the long-distance calculations done by tsunami propagation codes.

ACKNOWLEDGEMENTS

The SAGE code is a joint product of Los Alamos National Laboratory and Science Applications International, developed under the auspices of the Department of Energy's program in Advanced Simulation and Computing. We acknowledge very useful conversations with Charles Mader, Laura Kong, Frank Ham, Simon Day, and Steven Ward.

REFERENCES

D. K. Chester, "The 1755 Lisbon earthquake", *Progress in Physical Geography,* **25**, 363-383, 2001.

Gareth S. Collins & H. Jay Melosh, "Acoustic fluidization and the extraordinary mobility of sturzstroms", *Journal of Geophysical Research*, **108** (B10), 2473 doi:10.1029/2003JB002465, 2003.

Galen Gisler, Robert Weaver, Charles Mader, & Michael Gittings, "Two- and Three-Dimensional simulations of asteroid ocean impacts", *Science of Tsunami Hazards*, **21**, 119, 2003.

Charles L. Mader & Michael L. Gittings, "Modeling the 1958 Lituya Bay mega msunami, II", *Science of Tsunami Hazards*, **20**, 241, 2002.

Charles L. Mader, "Modeling the 1755 Lisbon tsunami", *Science of Tsunami Hazards*, **19**, 93, 2001.

Charles L. Mader, "Modeling the La Palma landslide tsunami", *Science of Tsunami Hazards*, **19**, 160, 2001.

M. S. Smith & J. B. Shepherd, "Potential Cauchy-Poisson waves generated by submarine eruptions of Kick 'em Jenny volcano", *Natural Hazards* **11**, 75-94, 1995.

George Pararas-Carayannis, "Evaluation of the threat of mega tsunamis generation from postulated massive slope failures of island stratovolcanoes on La Palma, Canary Islands, and on the island of Hawaii", *Science of Tsunami Hazards*, **20**, 251, 2002.

M. S. Smith & J. B. Shepherd, "Preliminary investigations of the tsunami hazard of Kick 'em Jenny submarine volcano", *Natural Hazards* **7**, 257-277, 1993.

Steven N. Ward & Simon Day, "Cumbre Vieja Volcano — potential collapse and tsunami at La Palma, Canary

Islands", *Geophysical Research Letters* **28**, 397-400, 2001.

Steven N. Ward & Simon Day, "Ritter Island Volcano — lateral collapse and the tsunami of 1888", *Geophysical Journal International*, **154**, 891-902, 2003.

R. B. Wynn & D. G. Masson, "Canary Island landslides and tsunami generation: can we use turbidite deposits to interpret lansdlide processes?" pp325-332 in: *Submarine Mass Movements and their Consequences* (eds. J. Locat and J. Mienert). Kluwer Academic Publishers, Dordrecht, Boston, London, 2003.